J Radioanal Nucl Chem (2013) 295:1487–1493
DOI 10.1007/s10967-012-2286-9

Quantifying the geometry correction factor and effectiveness parameter for Bonner sphere spectrometer with ^{3}He counter

Rahim Khabaz · Reza Izadi Najafabadi

Received: 20 June 2012

Abstract This paper presents the evaluation of the geometry correction factor for calibration of Bonner sphere spectrometer (BSS) equipped with the ^{3}He counter (typical SP9), based on Monte Carlo simulation. Using the MCNP4C code, geometry factors and effectiveness parameters (δ) of a 8″ polyethylene sphere ($r = 10.16$ cm) were calculated for 10 different energies and 3 various distances between the source and center of the sphere. The obtained results showed that the geometry factor increases with the distance, and the effectiveness parameter is independent of distance. Finally, for 2″, 3″, 5″, 8″ and 12″ spheres exposed to four different radio-isotopic neutron sources with various energy spectrums, the effectiveness parameters were determined, which it is worthy to consider $\delta \equiv \delta(r, E)$.

Keywords Neutron spectrometry · Bonner sphere · Calibration · Geometry factor · Effectiveness parameter · Monte Carlo

Introduction

Various systems have been developed for neutron spectrometry; the most commonly used are based on threshold detectors (activation or fission), ^{3}He proportional counters, LiI scintillators with ^{6}Li, proton recoil detectors, and the time-of-flight method [1].

Among many types of neutron spectrometers that have been developed, the system known as the multi-sphere, or more commonly, Bonner sphere spectrometer (BSS), has been built and used by more laboratories all over the world than any other type of spectrometer available [2, 3]. It consists of a thermal detector, a set of moderator spheres and associated electronics in the case of an active detector like BF$_3$, ^{3}He or ^{6}LiI(Eu) scintillator [4–8]. Several passive systems have been built, e.g. those utilizing gold foils or TLD pairs, too [9–11]. The BSS characterizes the neutron field from thermal to GeV [12].

The device readout depends upon the experimental features, such as, the energy spectrum and emission rate of the neutron source, the source encapsulation, the source-to-detector distance, and the size and layout of the irradiation area. Determination of the effect of these factors is specially important for facilities performing instrument calibrations to high precision and accuracy.

For a point-like detector and isotropic point-like source in an empty space, the product Ml^2 is a constant, where M is the dead-time corrected count rate of the detector, induced by the source at a separation distance l. This product is sometimes called the characteristic constant for the particular source-detector combination. A general functional relationship to the detector reading in open geometry, $M(l)$, at a separation distance between the neutron source and center of BSS, l, is given by the following equation:

$$M(l) = R_{\Phi} \frac{Q}{4\pi l^2} F(\theta)\, F_{\mathrm{s}}(l)\, F_1(l) \tag{1}$$

where R_{Φ} is the fluence response of the instrument; Q is the absolute emission rate of neutron source (i.e. emission rate

---

R. Khabaz (✉)
Physics Department, Faculty of Sciences, Golestan University, 49138-15739 Gorgan, Iran
e-mail: r.khabaz@gu.ac.ir; ra_khabaz@yahoo.com

R. I. Najafabadi
Physics Department, School of Sciences, Ferdowsi University of Mashhad, 91775-1436 Mashhad, Iran

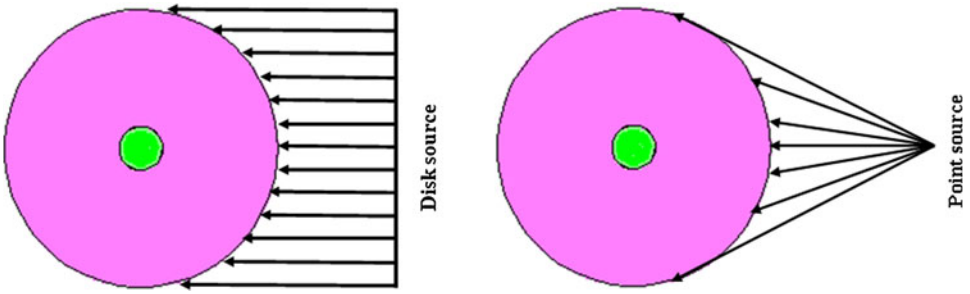

Fig. 1 Schematic of simulated BSS equipped with ^{3}He undergoing irradiation by plane-parallel and divergent neutron sources

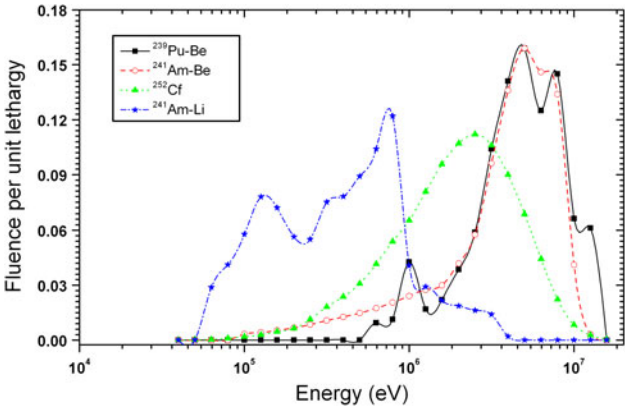

Fig. 2 Neutron spectra of ^{239}Pu–Be, ^{241}Am–Be, ^{252}Cf and ^{241}Am–Li neutron sources [21]

into 4π sr); $F(\theta)$ is the anisotropy factor for emission of source (influenced by the encapsulation and source type); $F_s(l)$ is the total air and room scattering correction factor; and $F_1(l)$ is the geometry correction factor (influenced by the source-detector distance, the source size and the detector size) that represents the departure from inverse square law [13, 14].

In order to calibrate a spherical device, all of the above factors need to be taken into consideration, and the result should be a value for the detector response that is independent of the experimental conditions.

While the detector is brought closer to the neutron source, the readings exceed those expected based on the inverse square law. The over-read increases to a maximum when the detector and the neutron source are in contact.

For a BSS and a point-like isotropic neutron source, Axton showed, through geometrical analysis of the system, that the response of the instrument in the center of sphere is increased by a factor of approximately $(1 + r^2/4l^2)$ above that expected according to the inverse square law, where r is the radius of the sphere, and l is the distance between the geometric centers of the source and detector [15]. The term $r^2/4l^2$ is the additional fractional number of neutrons entering the thermal counter. In the above analysis assumes that a point counter is placed in the center of sphere, although in practice, the thermal counters have size and volume. Axton suggested that it would be more realistic to fit data to $(1 + \delta r^2/4l^2)$, where the parameter δ attempts to account for the relative effectiveness of these extra neutrons in producing a response in the detector. Axton reasoned that δ is probably energy dependent, but independent of r/l and should have a value between 0 and 1. Then, Harrison extended it to the first three terms, and demonstrated, using the Monte Carlo method, that these conclusions are substantially correct, even for instruments with a relatively large counter, such as ^{3}He spherical counter having a diameter of 3.2 cm, at the center to detect the thermal neutrons [16]. The exact form of the geometry correction for an isotropic source, that originally published by Hunt [17], takes the form:

$$F_1(l) = 1 + \delta\left\{\frac{2l^2}{r^2}\left[1 - \left(1 - \frac{r^2}{l^2}\right)^{1/2}\right] - 1\right\}. \qquad (2)$$

The response of BSS as an ideal device, for radiation protection is defined by the ICRP [18] in terms of plane-parallel beams of neutrons. The geometry correction factor, $F_1(l)$, can be quantified by dividing the measured response of BSS under plane-parallel beam to the response of BSS under divergent beam conditions. The plane-parallel beams cannot be performed experimentally, except artificially when the device is itself scanned across a narrow collimated beam. Nowadays, with developed neutron transport and to the well evaluated nuclear cross-sections, determination of responses of any instrument under plane-parallel and divergent beams can be done by using the Monte Carlo method.

In this study, for a 8 in. ($r = 10.16$ cm) polyethylene sphere equipped with a ^{3}He proportional counter (typical SP9), the geometry factor and effectiveness parameter (δ) were determined for 10 different neutron energies, by Monte Carlo calculations using the computer code MCNP4C with ENDF/B-VI-0 neutron cross-section library. Also, the modeling of thermal neutron scattering due to chemical binding and crystalline effects in the polyethylene was considered with additional $S(\alpha, \beta)$ cross section tables available in the cross section library used [19].

Table 1 Calculated responses for 8″ sphere in diverging and parallel beams, as point source was placed at 15 cm from the center of sphere

Neutron energy (MeV)	Response of divergent beam (cm^2)	Error	Response of plane-parallel (cm^2)	Error	$F_1(l)$	Error	δ	Error
2.50E−08	1.3161E−01	2.3579E−04	1.1625E−01	1.5113E−04	1.1321	0.0035	0.8672	0.0230
3.16E−06	5.0504E−01	7.5755E−04	4.5125E−01	4.9638E−04	1.1192	0.0029	0.7826	0.0191
5.00E−04	8.0432E−01	1.0456E−03	7.1704E−01	6.4534E−04	1.1217	0.0025	0.7993	0.0162
2.00E−03	8.8272E−01	1.0593E − 03	7.8531E−01	7.0678E−04	1.1240	0.0024	0.8146	0.0155
2.40E−02	1.0689E+00	1.1758E−03	9.5131E−01	7.6105E−04	1.1236	0.0021	0.8115	0.0140
5.65E−01	2.3126E+00	1.8501E−03	2.0898E+00	1.4628E−03	1.1066	0.0017	0.7003	0.0109
1.20E+00	2.7578E+00	2.2062E−03	2.5059E+00	1.7541E−03	1.1005	0.0017	0.6600	0.0108
5.00E+00	2.1447E+00	1.9302E−03	1.9580E+00	1.3706E−03	1.0953	0.0018	0.6258	0.0115
1.20E+01	1.1681E+00	1.4018E−03	1.0668E+00	8.5341E−04	1.0950	0.0022	0.6240	0.0144
1.80E+01	8.6019E−01	1.2043E−03	7.8683E−01	7.8683E−04	1.0932	0.0026	0.6122	0.0172

Table 2 Calculated responses for 8″ sphere in diverging and parallel beams, as point source was placed at 20 cm from the center of sphere

Neutron energy (MeV)	Response of divergent beam (cm^2)	Error	Response of plane-parallel (cm^2)	Error	$F_1(l)$	Error	δ	Error
2.50E−08	1.2354E−01	1.3002E−04	1.1625E−01	1.5113E−04	1.0627	0.0025	0.8413	0.0339
3.16E−06	4.7697E−01	4.2295E−04	4.5125E−01	4.9638E−04	1.0570	0.0021	0.7653	0.0277
5.00E−04	7.6112E−01	7.4903E−04	7.1704E−01	6.4534E−04	1.0615	0.0020	0.8256	0.0271
2.00E−03	8.3385E−01	7.4164E−04	7.8531E−01	7.0678E−04	1.0618	0.0019	0.8295	0.0256
2.40E−02	1.0089E+00	1.0004E−03	9.5131E−01	7.6105E−04	1.0605	0.0019	0.8121	0.0249
5.65E−01	2.2030E+00	2.2195E−03	2.0898E+00	1.4628E−03	1.0542	0.0018	0.7283	0.0246
1.20E+00	2.6340E+00	2.1657E−03	2.5059E+00	1.7541E−03	1.0511	0.0016	0.6861	0.0221
5.00E+00	2.0493E+00	1.1110E−03	1.9580E+00	1.3706E−03	1.0466	0.0013	0.6255	0.0169
1.20E+01	1.1173E+00	1.0263E−03	1.0668E+00	8.5341E−04	1.0474	0.0018	0.6367	0.0245
1.80E+01	8.2154E−01	9.8819E−04	7.8683E−01	7.8683E−04	1.0441	0.0023	0.5922	0.0307

Furthermore, the simulation was carried out for four radio-isotopic neutron sources that have different energy spectra, i.e. ^{239}Pu–Be, ^{241}Am–Be, ^{252}Cf and ^{241}Am–Li sources, to evaluate the geometry factors and effectiveness parameters of ^{3}He detector placed inside 2, 3, 5, 8 and 12-inch diameter moderating spheres composed of polyethylene.

Materials and method

Since for the calibration through radionuclide neutron sources, the source usually approximates to a point, so in MCNP simulation for calculation of the response of BSS under divergent beams, the source was defined as a point-like neutron source. Also, in the case of plane-parallel beams, the irradiation geometry was based on a disk source with the same diameter of the sphere under study. Source-term neutrons were parallel to the source-detector axis and fully included the entire surface of the moderating sphere, as is shown in Fig. 1.

At the first step, the calculation of responses to neutrons was done for a highly sensitive ^{3}He spherical proportional counter with 3.2 cm diameter (typical SP9), placed in the centre of a polyethylene sphere (by density of 0.96 g/cm^3) with an outer diameter of 8 inches.

The gas pressure in the counter model was 172 kPa (1.697 atm) resulting in an atom density, at 293 K, of 4.2497×10^{-5} atom/barn.cm. The ^{3}He counter wall is made of Monel alloy with 0.3 mm-thick and 8.6 g/cm^3 density whose weight fraction of element composition is 64.86 % Ni, 30.24 % Cu, 2.44 % Fe, 1.95 % Mn, 0.49 % Si and 0.02 % S [20]. In the model the counter wire was not included.

The calculation of responses to neutrons was for moderator–detector configuration, with mono-energetic neutron beam of 10 different energies that were extended from thermal to 18 MeV in energy. Discrete neutron energy values were selected at logarithmic equidistant intervals and at decade boundaries [6, 20].

The calculation of the response was accomplished by selecting the tally F4 of MCNP4C, the (n, p) reaction being

Table 3 Calculated responses for 8″ sphere in diverging and parallel beams, as point source was placed at 25 cm from the center of sphere

Neutron energy (MeV)	Response of divergent beam (cm^2)	Error	Response of plane-parallel (cm^2)	Error	$F_1(l)$	Error	δ	Error
2.50E−08	1.2061E−01	6.4078E−05	1.1625E−01	1.5113E−04	1.0375	0.0019	0.8313	0.0421
3.16E−06	4.6662E−01	2.0869E−04	4.5125E−01	4.9638E−04	1.0341	0.0016	0.7553	0.0345
5.00E−04	7.4342E−01	6.2158E−04	7.1704E−01	6.4534E−04	1.0368	0.0018	0.8156	0.0391
2.00E−03	8.1516E−01	6.0140E−04	7.8531E−01	7.0678E−04	1.0380	0.0017	0.8430	0.0382
2.40E−02	9.8726E−01	8.2740E−04	9.5131E−01	7.6105E−04	1.0378	0.0017	0.8378	0.0367
5.65E−01	2.1598E+00	1.6229E−03	2.0898E+00	1.4628E−03	1.0335	0.0015	0.7435	0.0341
1.20E+00	2.5848E+00	1.6989E−03	2.5059E+00	1.7541E−03	1.0315	0.0014	0.6984	0.0311
5.00E+00	2.0122E+00	1.5284E−03	1.9580E+00	1.3706E−03	1.0277	0.0015	0.6138	0.0331
1.20E+01	1.0982E+00	8.2824E−04	1.0668E+00	8.5341E−04	1.0295	0.0016	0.6535	0.0360
1.80E+01	8.0755E−01	6.0879E−04	7.8683E−01	7.8683E−04	1.0263	0.0018	0.5838	0.0398

considered, associated to a card multiplier (FMn card) that for responses under divergent beams contains the volume of the detector, the atom density (atom/barn.cm) of ^{3}He, and the area of a sphere with radius equal to distance between the source and the center of BSS (l); and for plane-parallel beams, this card multiplier contains the volume of the detector, atom density counter, and the area of the disk source. The final output of MCNP calculation was in terms of cm^2. These calculations were performed for three different distances between the point mono-energetic neutron source and the center of BSS (l), i.e. 15, 20 and 25 cm.

Finally, for some radio-isotopic neutron sources such as ^{239}Pu–Be with a mean energy about 5.40 MeV, ^{241}Am–Be with a mean energy about 4.46 MeV, ^{252}Cf with a mean energy about 2.54 MeV, and ^{241}Am–Li with a mean energy about 0.56 MeV, the divergent and plane-parallel beams responses of the BSS with diameters of 2″, 3″, 5″, 8″ and 12″ that surrounds the ^{3}He counter (typical SP9) were calculated. The neutron spectrum of these radionuclide neutron sources are shown in Fig. 2 [21]. For determination of all responses, the calculations were performed up to appropriate histories, which provide a reasonable statistical error.

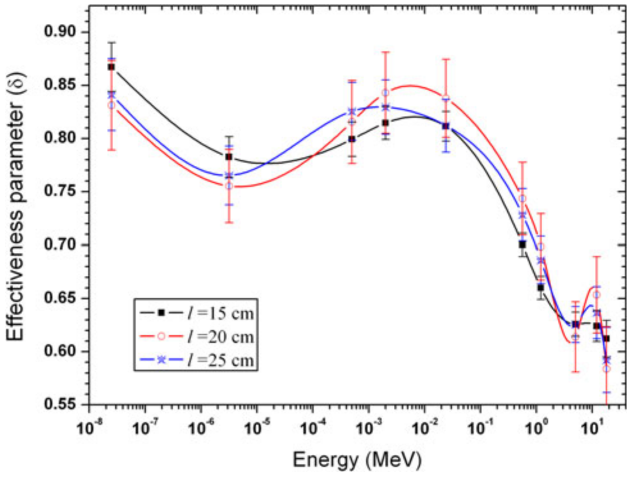

Fig. 3 Calculated effectiveness parameters versus the neutron energy for various l

Results and discussion

The responses of a 8 inches ($r = 10.16$ cm) polyethylene sphere equipped with a ^{3}He proportional counters undergoing irradiation by plane-parallel and divergent neutron sources were calculated for 10 various energies from 2.5×10^{-8} to 18 MeV. For divergent beams, the point neutron sources were placed at three different distances from the center of sphere, i.e., 15, 20 and 25 cm.

Tables 1, 2 and 3 present the numerical values associated with statistical errors for the plane-parallel and divergent beams. The effect of irradiation geometry, $F_1(l)$, was obtained simply by determining the ratio of divergent to the plane-parallel beam response. Also, by putting the values of r and l in Eq. 2 and using the geometry factor acquired from the Monte Carlo calculations can achieve to the effectiveness parameter (δ).

From comparison of the results of Tables 1, 2 and 3 is obvious that geometry factor for each energy decreases with increasing distance (l).

The effectiveness parameters with error bar are plotted in Fig. 3 as a function of neutron energy for three different distances obtained from the calculations.

As it can be seen, the effectiveness parameters for a 8″ sphere are functions of the neutron energy and approximately independent of the distance (l). A little difference for various distances at each energy value may be due to the statistical uncertainty in Monte Carlo calculation. In this figure the effectiveness parameters vary from about

Table 4 Numerical values of the responses of the BSS with ^{3}He exposed to divergent and parallel beams of ^{239}Pu–Be source associated with calculated geometry factors

Sphere diameter	Response of divergent beam (cm^2)	Error	Response of plane-parallel (cm^2)	Error	$F_1(l)$	Error	δ	Error
2 in.	7.0931E−03	2.5868E−05	6.7011E−03	8.7114E−06	1.0585	0.0052	0.7854	0.0625
3 in.	1.6652E−01	1.9982E−04	1.4312E−01	7.1560E−05	1.1635	0.0020	0.7644	0.0092
5 in.	1.1203E+00	1.0083E−03	1.0261E+00	3.0783E−04	1.0918	0.0013	0.7153	0.0102
8 in.	2.1579E+00	1.9421E−03	1.9592E+00	9.7960E−04	1.1014	0.0015	0.6660	0.0101
12 in.	1.8413E+00	2.2096E−03	1.6523E+00	1.8175E−03	1.1144	0.0026	0.5348	0.0120

Table 5 Numerical values of the responses of the BSS with ^{3}He exposed to divergent and parallel beams of ^{241}Am–Be source associated with calculated geometry factors

Sphere diameter	Response of divergent beam (cm^2)	Error	Response of plane-parallel (cm^2)	Error	$F_1(l)$	Error	δ	Error
2 in.	4.5324E−03	1.5043E−05	4.2574E−03	6.8118E−06	1.0646	0.0052	0.8672	0.0703
3 in.	1.1827E−01	1.6558E−04	1.0185E−01	6.1110E−05	1.1612	0.0023	0.7537	0.0109
5 in.	9.1266E−01	9.1266E−04	8.3687E−01	2.5106E−04	1.0906	0.0014	0.7056	0.0110
8 in.	1.9999E+00	1.7999E−03	1.8245E+00	7.2980E−04	1.0961	0.0014	0.6313	0.0094
12 in.	1.9531E+00	2.3437E−03	1.7492E+00	1.2244E−03	1.1166	0.0021	0.5450	0.0099

Table 6 Numerical values of the responses of the BSS with ^{3}He exposed to divergent and parallel beams of ^{252}Cf source associated with calculated geometry factors

Sphere diameter	Response of ivergent beam (cm^2)	Error	Response of plane-parallel (cm^2)	Error	$F_1(l)$	Error	δ	Error
2 in.	1.9975E−02	5.9925E−05	1.8750E−02	1.5000E−05	1.0653	0.0040	0.8771	0.0544
3 in.	3.6006E−01	2.8805E−04	3.0909E−01	9.2727E−05	1.1649	0.0013	0.7709	0.0060
5 in.	1.7646E+00	1.2352E−03	1.6127E+00	4.8381E−04	1.0942	0.0011	0.7339	0.0085
8 in.	2.4494E+00	1.9595E−03	2.2259E+00	1.3355E−03	1.1004	0.0015	0.6593	0.0101
12 in.	1.4525E+00	2.0335E−03	1.2992E+00	1.8189E−03	1.1180	0.0031	0.5516	0.0146

Table 7 Numerical values of the responses of the BSS with ^{3}He exposed to divergent and parallel beams of ^{241}Am–Li source associated with calculated geometry factors

Sphere diameter	Response of divergent beam (cm^2)	Error	Response of plane-parallel (cm^2)	Error	$F_1(l)$	Error	δ	Error
2 in.	6.8879E−02	1.1021E−04	6.4417E−02	2.5767E−05	1.0693	0.0021	0.9300	0.0287
3 in.	8.3563E−01	4.1782E−04	7.1484E−01	1.4297E−04	1.1690	0.0008	0.7900	0.0038
5 in.	2.5049E+00	1.5029E−03	2.2808E+00	6.8424E−04	1.0983	0.0010	0.7656	0.0077
8 in.	1.9655E+00	1.7690E−03	1.7741E+00	1.0645E−03	1.1079	0.0017	0.7084	0.0109
12 in.	5.5976E−01	1.1755E−03	4.9402E−01	8.8924E−04	1.1331	0.0044	0.6221	0.0207

0.58 to 0.87. The obtained results properly confirm the arguments presented by Axton [15].

Among different neutron fields, the radionuclide neutron sources are the most important in the calibration of BSS. Therefore the δ for such sources will be different because the effectiveness parameter depends upon the neutron energy. Each radionuclide neutron source has their own energy spectrum that their mean energy is about from few tenths to few MeV.

In this work, the effect of the irradiation geometry was calculated for 2″, 3″, 5″, 8″ and 12″ polyethylene spheres exposed to ^{239}Pu–Be, ^{241}Am–Be, ^{252}Cf and ^{241}Am–Li neutron sources with different mean energies. These neutron sources and sphere diameters were chosen to represent adequately all neutron energies and all sphere sizes.

Since, the effectiveness parameter was independent of *l*, so to minimize the statistical error in the calculation of diverging beam, distance of point source to center of the sphere was considered 5, 5, 10, 15 and 20 cm for 2″, 3″, 5″, 8″ and 12″ spheres, respectively.

The computational values associated with statistical errors for different spheres undergoing irradiation by the plane-parallel and divergent beams of ^{239}Pu–Be, ^{241}Am–Be, ^{252}Cf and ^{241}Am–Li neutron sources and geometry factors of each condition are listed in Tables 4, 5, 6 and 7, respectively.

It can be seen that effectiveness parameters, δ, for each set of sphere size and neutron source is different. Therefore, it is worthy to consider $\delta \equiv \delta(r, E)$. For all sources, effectiveness parameter decreases with increasing the diameter of sphere. The maximum and minimum values of δ are for 2″ sphere exposed to ^{241}Am–Li and 12″ sphere exposed to ^{239}Pu–Be neutron source, respectively.

Conclusions

The BSS is widely used for radiation protection purposes, during its calibration several correction factors need to be determined. One of them is the geometry correction factor which is related to the non-uniform illumination of the spectrometer at short distances giving rise to serious departures from the inverse square law. Since, experimental measurement of this factor is associated with some technical problems, so the Monte Carlo calculation can be a suitable method to obtain it. Then, the geometry factor of BSS with ^{3}He counter was evaluated based on MCNP modeling.

It is concluded from the comparison of the results of calculation by MCNP4C for the 8″ polyethylene sphere that the geometry factor increases with decreasing the distance of neutron source and center of sphere, and has a greater impact on the instrument calibration. The effectiveness parameter, δ, obtained by simulations, as Axton had already argued, was dependent of energy and independent of *r/l*. Therefore, this parameter was calculated for several sources with different spectra that can be used in calibration of BSS. The δ was different for any set of sphere diameter and neutron source, and had a value between 0 and 1; then it can be considered equivalent with $\delta(r, E)$. The average value of δ for all spheres was 0.6932 ± 0.0208, 0.7006 ± 0.0223, 0.7186 ± 0.0187 and 0.7632 ± 0.0144 for ^{239}Pu–Be, ^{241}Am–Be, ^{252}Cf and ^{241}Am–Li neutron sources, respectively. These values are approximately close to the suggested value by Axton [15], i.e. to a value of 2/3 for all sphere sizes and energies.

This Monte Carlo study can be generalized to obtain the values of geometry correction factor and the effectiveness parameter of BSS with another thermal neutron detectors and different neutron sources.

References

1. Nakamura T (2003) Recent development of advanced neutron detection technology. J Nucl Radiochem Sci 4:15–24
2. Vega-Carrillo HR et al (2009) Spectra and dose with ANN of ^{252}Cf, ^{241}Am–Be, and ^{239}Pu–Be. J Radioanal Nucl Chem 281:615–618
3. Thomas DJ, Alevra AV (2002) Bonner sphere spectrometers-a critical review. Nucl Instrum Methods A 476:12–20
4. Khabaz R, Miri H (2011) Measurement of neutron spectrum with multi-sphere using BF$_3$ and evaluation of scattering effect on spectrum. Nucl Technol Radiat Prot 26:140–146
5. Khabaz R, Miri H (2011) Determination of ^{241}Am–Be spectra using Bonner sphere spectrometer by applying shadow cone technique in calibration. J Appl Sci 11:2849–2854
6. Khabaz R (2012) Study of a new multi-sphere spectrometer based on water moderator with a high efficiency ^{6}LiI(Eu) detector. J Radioanal Nucl Chem 293:383–389
7. Hakim M et al (2008) Characterization of the CRNA Bonner sphere spectrometer based on LiI scintillator exposed to an Am–Be neutron source. Radiat Meas 43:1095–1099
8. Hakim M, Zahir I, Tassadit S, Malika A (2010) MCNP5 evaluation of a response matrix of a Bonner sphere spectrometer with a high efficiency ^{6}LiI (Eu) detector from 0.01 to 20 MeV neutron. J Radioanal Nucl Chem 284:253–263
9. Tripathy SP et al (2009) Measurement of ^{241}Am–Be spectra (bare and Pb-covered) using TLD pairs in multi-spheres: spectrum unfolding by different methods. Nucl Instrum Methods A 598: 556–560
10. Vega-Carrillo HR (2002) TLD pairs, as thermal neutron detectors in neutron multisphere spectrometry. Radiat Meas 35(251):254
11. Vega-Carrillo HR, Hernandez-Almaraz B, Hernandez-Davila VM, Montalvo TR, Ortiz-Hernandez A (2010) Neutron spectrum and doses in a 18 MV LINAC. J Radioanal Nucl Chem 283:261–265
12. Wiegel B, Alevra AV (2002) NEMUS—the PTB neutron multisphere spectrometer: bonner spheres and more. Nucl Instrum Methods 476:36–41
13. Khabaz R, Miri H (2011) Development of a Bonner sphere spectrometer with emphasis on decreasing the contribution of scattering by using a new designed shadow cone. J Radioanal Nucl Chem 289:789–794
14. Taylor GC (2010) Geometry corrections for cylindrical neutron area survey meters. Appl Radiat Isot 68:546–549
15. Axton EJ (1972) The effective centre of a moderating sphere when used as an instrument for fast neutron flux measurement. J Nucl Energy 26:581–583
16. Harrison KG (1981) The calibration of neutron detectors with spherical moderators. Nucl Instrum Methods 184:595–597
17. Hunt JB (1984) The calibration of neutron sensitive spherical devices. Radiat Prot Dosimetry 8:239–251
18. ICRP (1973) Data for protection against ionizing radiation from external sources. ICRP Publication 21, Pergamon Press, Oxford

19. Briesmeister JF (2000) MCNP-a general Monte Carlo N-particle transport code, Version 4C. Los Alamos National Laboratory Report LA-13709-M, Los Alamos
20. Khabaz R, Miri H (2011) Evaluation of response matrix of a multisphere neutron spectrometer with water moderator. PRAMANA J Phys 77:599–609
21. Griffith RV, Palfalvi J, Madhvanath U (1990) Compendium of neutron spectra and detector responses for radiation protection purposes. International Atomic Energy Agency, Technical Report Series No. 318